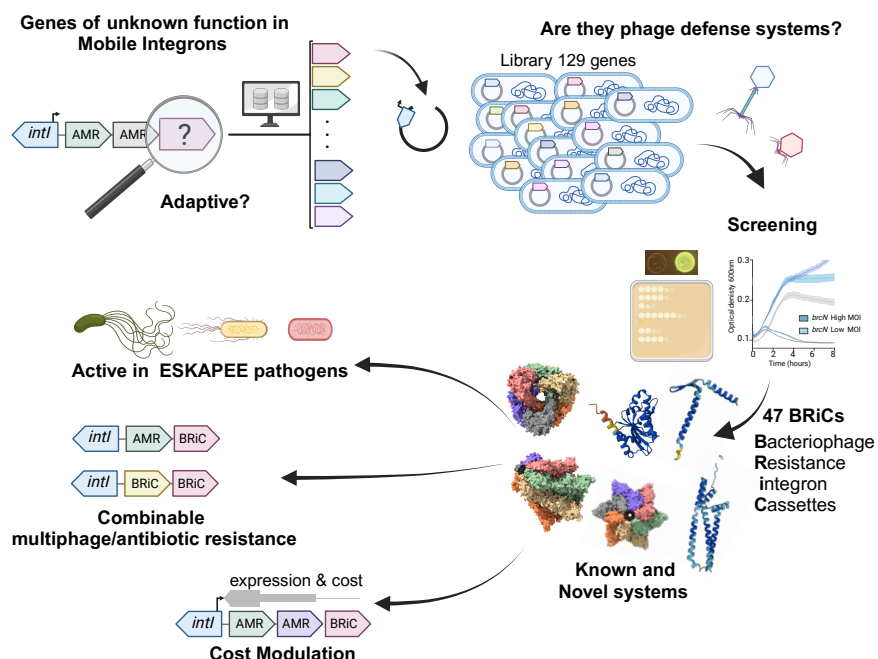


36 **Abstract: Integrons are bacterial genetic elements that capture, stockpile and modulate the**
37 **expression of genes encoded in integron cassettes. Mobile Integrins (MI) are borne on**
38 **plasmids, acting as a vehicle for hundreds of antimicrobial resistance genes among key**
39 **pathogens. These elements also carry gene cassettes of unknown function (gcus) whose role**
40 **and adaptive value remains unexplored. Here we show that gcus encode phage resistance**
41 **systems, many of which are novel. Bacteriophage resistance integron cassettes (BRiCs) can**
42 **be combined and mixed with resistance cassettes to produce multiphage or drug/phage-**
43 **resistance. The fitness costs of BRiCs are variable, dependent on the genetic context, and can**
44 **be modulated by changing the order of cassettes in the array. Hence, MIs act as highly mobile,**
45 **low-cost defense islands.**



46
47 **Summary Figure: Novel phage defense systems identified in Mobile Integrins.** We confronted genes of unknown
48 function from mobile integrins against a panel of phage. We characterized 13 Bacteriophage Resistance integron
49 Cassettes (BRiCs) and confirmed their function in *Klebsiella pneumoniae* and *Pseudomonas aeruginosa*. Combined
50 with other cassettes, BRiCs produce multi-phage/antibiotic resistance. Additionally, their cost can be reduced in an
51 array.

52
53
54
55
56
57
58
59

60 **Main Text:**
61 **INTRODUCTION**

62 Antimicrobial resistance (AMR) is a major public health concern worldwide, and the
63 emergence of multi-drug (MDR) resistant bacteria is making increasingly difficult to treat
64 infections with antibiotics (1). Phage therapy -the use of viruses that infect and kill bacteria- is
65 currently building momentum as an alternative to antibiotics (2–4). However, its efficacy can be
66 limited too by the emergence of resistance (5, 6). In recent years, a plethora of new phage defense
67 systems (PDSs) have been discovered (7), often co-localizing in defense islands (8–10). Some
68 PDSs are encoded in mobile genetic elements (MGEs) such as integrative conjugative elements,
69 transposons, or prophages (11). While their spread is a threat to phage therapy, PDSs can entail a
70 fitness cost to their host limiting their dissemination (12).

71 Integrins are genetic elements that play an important role in bacterial adaptation to
72 changing environmental conditions (13–15). They capture and accumulate new genes embedded
73 in integron cassettes (ICs), acting as genetic memories of adaptive functions (16). Integrins
74 typically consist of a conserved platform encoding the integrase gene and the recombination site in
75 the integron (*attI*) (17); and a variable region containing the cassettes. Cassettes are incorporated
76 into the *attI* site through site-specific recombination reactions mediated by the integrase and are
77 expressed from the dedicated *Pc* promoter encoded in the platform (18). The integrase can also
78 reorder cassettes in the array to modulate their expression, modifying their distance to the *Pc* and
79 the polar effects they are subjected to (19–21). The expression of the integrase is controlled by the
80 SOS response, so that integrins provide to their hosts adaptation on demand (22, 23). MIs are a
81 subset of integrins associated with plasmids and transposons, that facilitate their transfer between
82 bacterial cells (24–26). They are currently commonplace among key Gram-negative pathogens (27)
83 carrying almost 200 resistance genes against most antibiotic families (28–30). Although generally
84 devoted to AMR, MIs also carry gene cassettes of unknown function (*gcus*), whose importance has
85 commonly been overlooked. The working model of integrins suggests that cassettes must be
86 adaptive at the time of integration (22). Given the importance of phage predation in the lifestyle of
87 bacteria, we sought to explore if *gcus* encode phage defense systems.

88 We have selected 129 non-redundant *gcus* from the INTEGRALL database (31), and cloned
89 them as cassettes in a mobile integron (30). DefenseFinder (32) and PADLOC (33) predicted
90 potential defense systems in 4 *gcus* in this collection. Screening the library against a panel of phage,
91 we found 43 novel defense systems. We have characterized 13 systems further and confirmed that
92 they are encoded in functional integron cassettes, which we have named Bacteriophage Resistance
93 integron Cassettes (BRiCs). They are hence mobile and exchangeable between integron platforms
94 that circulate among many species. We demonstrate that they also confer protection in *K.*
95 *pneumoniae* and *P. aeruginosa*, major pathogens of the ESKAPEE group. As part of an integron,
96 defense systems can be stockpiled in an array where their position allows to modulate their function
97 and strongly diminish their cost. We also show that phenotypes encoded in BRiCs are additive,
98 conferring multi-phage or phage/drug resistance if combined with other BRiCs or antimicrobial
99 resistance cassettes (ARCs). We discovered a natural example of a three-BRiC array, confirming
100 that multiphage resistance integrins are already present in clinical isolates. Altogether, our work
101 shows the involvement of integrins in phage defense, acting mobile and low-cost defense islands.

102

103

104

105

106

107 **RESULTS**

108

109 **Integron *gcus* contain predicted phage defense systems.**

110 To obtain a broad set of *gcus* in MIs we screened the INTEGRALL database (date:
111 November 2021) and elaborated a curated list of 129 *gcus* with < 95% nucleotide identity (Fig.
112 S1). We synthesized and cloned them in pMBA, as cassettes in first position of a class 1 MI under
113 the control of a strong *Pc* promoter (*PcS*) (30). The sequences of our selected collection were
114 submitted in May 2022 to DefenseFinder and PADLOC (32, 33) predicting that 4 cassettes (*gcu59*,
115 *gcu128*, *gcu135* and *gcuN*) contained homologs of known defense mechanisms (Fig. 1A).

116 Given their newly identified putative function as BRiCs, we propose to rename these *gcus*
117 as *brcs*, while conserving their initial numbers or letters for simplicity. *Brc59* (formerly *Gcu59*)
118 was identified as a homolog of the *AriAB* abortive infection system (34). *brc128* encodes two ORFs
119 (*brc128A* and *B*) showing similarity to Lamassu Type 1 systems. AlphaFold predicts that *Brc128A*
120 shares motifs with *YfjL*-like or *AbpA* proteins, involved in phage defense, while *Brc128B* contains
121 a putative exonuclease domain. *brc135* also contains two ORFs encoding proteins with roles in
122 nucleotidyl-transfer and membrane translocation and showing structural similarity with a CBASS
123 Type 1 system (35, 36). Last, *brcN* encodes an *AbiV* family protein (37), implicated in abortive
124 infection defense.

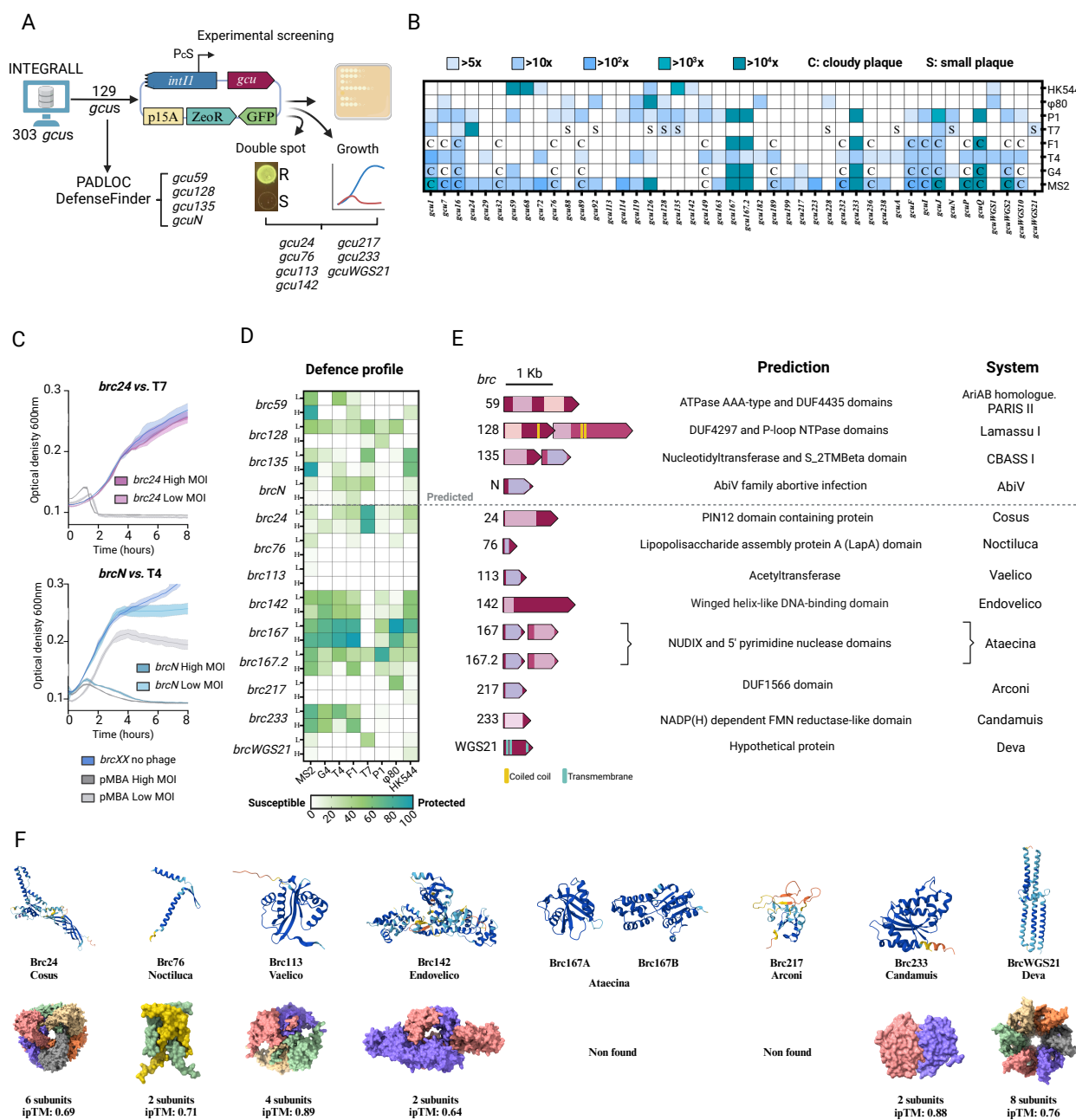
125

126 **Functional screening reveals additional phage defense systems.**

127 To search for novel PDSs that might not be detected by algorithms, we confronted
128 experimentally the whole *gcu* collection (established in DH5 α) against phages T4 or T7 using a
129 double-spot screening protocol and growth curve monitoring (Fig. 1A and S1). We successfully
130 detected 7 new candidates (*brc24*, *brc76*, *brc113*, *brc142*, *brc217*, *brc233* and *brcWGS21*) that
131 enabled growth in the presence of phage, suggesting that PDSs might be abundant among *gcus*. To
132 better address this, we subcloned the collection in strain *E. coli* IJ1862 (an F' strain that can be
133 infected by phages targeting the conjugative pilus (38)) and subjected it to plaque assays with
134 phages MS2, F1, G4, T4, T7, P1, Φ 80 and HK544. This screening revealed that 45 *gcus* in the
135 collection conferred >5-fold protection against at least one phage (Fig 1B). Because some
136 phenotypes -like cloudy plaques- are difficult to interpret and quantitate, we selected 13 systems
137 with clear phenotypes in the double-spot assay for further characterization, 9 of which are novel.
138 We conducted infection assays with all phages at varying multiplicities of infection (MOIs) and
139 monitored the optical densities (OD₆₀₀) of bacterial cultures over time (Fig. 1C). We used the area
140 under the growth curve compared to an empty vector control to determine the protective effect of
141 the cassette, as in (39) (see Materials and Methods). Our data confirmed that all BRiCs conferred
142 resistance to at least one phage at one MOI (Fig. 1D and Fig. S2). Resistance profiles were diverse,
143 with examples of broad-spectrum BRiCs, and others a narrower spectrum but very high resistance
144 against a given phage. The resistance conferred by *brcN* is limited to low MOIs confirming *in silico*
145 predictions of an abortive infection system. Overall, our results confirm that at least one third of
146 *gcus* are indeed phage resistance genes.

147 Structure modelling and domain predictions (Fig. 1E, 1F and S3) showed that most systems
148 are novel and many do not contain recognizable domains or are of unknown function. Instead,
149 about a third of BRiCs contained transmembrane helices, compatible with direct interference with
150 phage infection (Fig. 1E and S3). Among the predicted domains found, some have been previously
151 related to phage defense, like the Toll-Interleukin receptor in *Brc236* (40), or the toxin antitoxin
152 system (*HigAB*) in *Brc182* (41); while others have roles easily related to phage resistance (mRNA
153 splicing for *Brc232* or DNA repair for *Brc68*) (Fig. S3). Among the selected BRiCs, *Brc24*

154 possesses a PIN12 RNA-binding domain (42) and potentially acts as a hexameric protein. Brc76 is
 155 a small protein of 76 amino acid with a LapA domain related to biofilm formation and forms dimers
 156 (43). Brc113 has a GNAT N-acetyltransferase domain (also found in BrcP (Fig. S3)). Brc142 is a
 157 putative dimeric restriction endonuclease. *brc167* and its close homolog *brc167.2* encode proteins
 158 with NUDIX hydrolase and nucleotidase activities with no evident multimeric structure. Brc217
 159 contains the domain of unknown function (DUF) 1566 and no identified multimeric structure.
 160 Brc233 is possibly a dimeric NADP(H) oxidoreductase; and last, BrcWGS21 has no identified
 161 domains but contains transmembrane helices and conforms an octamer potentially forming a pore
 162 in the membrane. To adhere to the custom in the field, these novel systems are also given the name
 163 of a deity of Celtiberian mythology (Fig. 1E).



164

165 **Fig. 1. Identification and Characterization of Phage Defense Systems in Integron Cassettes.** (A) Schematic
166 workflow for detection of PDSs in *gcus*. A curated collection from INTEGRALL was cloned in pMBA vector. Systems
167 were identified using PADLOC and DefenseFinder, (May 2022), double-spot assays, growth curves and plaque assays.
168 (B) Profile against a panel of eight *E. coli* phages of *gcus* providing >5-fold defense against at least one phage. (C)
169 Examples of growth curves used to build the heatmap in C: *brc24* confers strong resistance to phage T7 at both high
170 and low MOI while *brcN* shows resistance to phage T4 only at low MOI. Growth curves are represented as the mean
171 of three independent replicates. The standard error of the mean is represented as a lighter color shade. (D) Heatmap
172 showing the defense profiles at different MOIs. The degree of protection (resistance) is indicated by the color scale,
173 with dark green representing high protection, light green representing low protection, and white no protection. (E)
174 Genetic organization and predicted functions of selected *gcus*. (F) Tertiary and quaternary structures of novel phage
175 defense systems, as predicted by AlphaFold3.

176

177 **BRiCs are *bona fide* integron cassettes.**

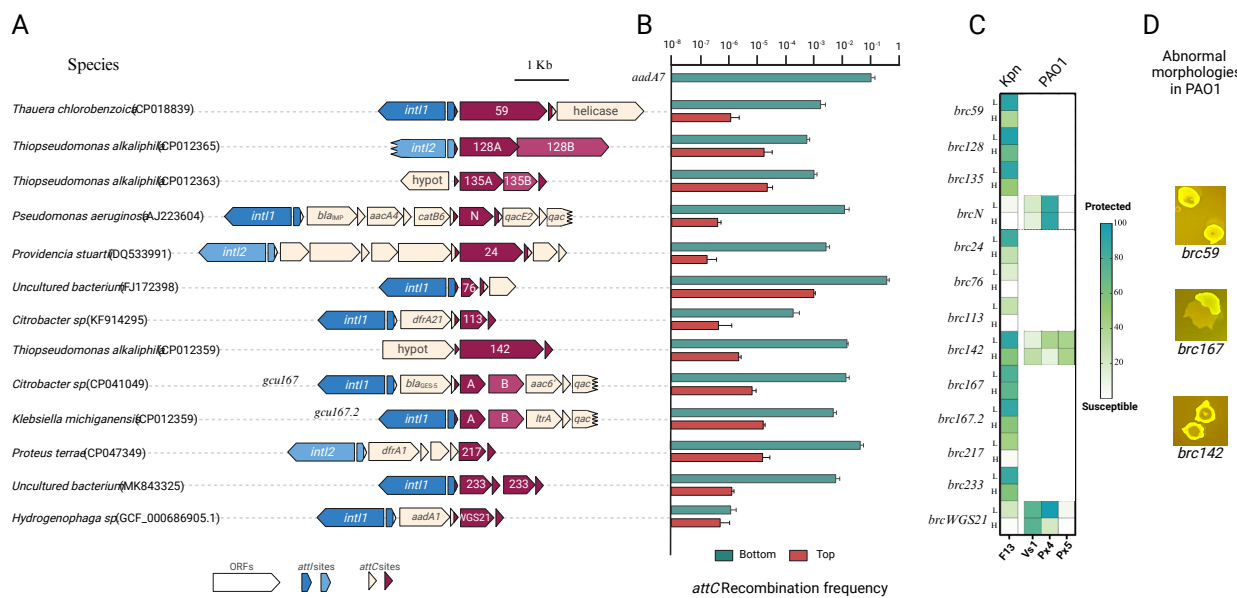
178 Finding defense systems in integron cassettes has important implications for the mobility
179 of these elements. Identification of cassettes has not been straightforward until the development of
180 IntegronFinder (44). INTEGRALL predates IntegronFinder. The genetic context, suggests that
181 most BRiCs identified here are indeed located within class 1 or 2 MIs, often in pathogenic and
182 multidrug resistant strains (like *brc217*, *brc113*, *brc24* or *brcN*) (Fig. 2A). But other, like *brc135*
183 and *brc142*, did not have an MI context. Hence we wanted to verify that PDSs are encoded in *bona*
184 *fide*-functional- integron cassettes. Integron recombination is semiconservative, involving only the
185 bottom strand of *attC* and *attI* sites (45, 46). This unique feature can be detected in a suicide
186 conjugation assay as the difference between recombination rates when the plasmid transfers the
187 bottom or the top strand of an *attC* site to the recipient strain (46). We measured this for all cassettes
188 and observed a 100- to 10.000-fold lower recombination of top strands (Fig. 2B). *brcWGS21* had
189 extremely low recombination frequencies for the bottom strand, yet recombination of the top strand
190 was only observed in 1 out of 6 replicate experiments, suggesting that it is probably an integron
191 cassette, albeit with a very poor recombination site. Accordingly, the folded *attC* site of *brcWGS21*
192 has the typical hairpin structure and extra-helical bases of these sites (Fig. S4) (46–48). Hence, our
193 data confirms that BRiCs are *bona fide* integron cassettes.

194

195 **Defense cassettes are protective in other species.**

196 Given the mobility of integrons and cassettes among important pathogens, we sought to
197 determine if BRiCs are active in different hosts. To this end, we evaluated their protective effect in
198 *K. pneumoniae* and *P. aeruginosa*, two species of the ESKAPEE group of highly resistant and lethal
199 pathogens where integrons are prevalent. We introduced all BRiCs into *K. pneumoniae* KP5, a
200 MDR clinical isolate that contains three plasmids (Fig. S5) and subjected them to infection with
201 phage F13, a *Drexlerviridae* member co-isolated with the strain. All BRiCs, except *brcN*,
202 demonstrated resistance to F13 at low MOI, and most also conferred resistance at high MOI (except
203 *brc76*, *brc113*, *brc217*, and *brcWGS21*) (Fig. 2C). To introduce BRiCs in *P. aeruginosa* PAO1
204 strain, we changed the p15A origin of replication of pMBA for BBR1, and introduced a tetracycline
205 resistance marker. After several assays, we could only transform *brcN* successfully, while other
206 BRiCs produced no colonies at all or abnormal colony morphologies (Fig. 2D). This led us to
207 hypothesize that some BRiCs might be toxic or extremely costly in this background. To avoid this,
208 we changed the *PcS* promoter driving the expression of cassettes for a weaker version (*PcW*, 30-
209 fold less active than the *PcS* (49)). This allowed to introduce *brc24*, *brc113*, *brc142* and *brcWGS21*
210 in PAO1. We confronted these strains to a collection of 36 phages infecting PAO1 using a double
211 spot screen. *brcN*, *brc142* and *brcWGS21* showed growth in presence of phages Vs1, Px4 and Px5.
212 We confirmed their resistance phenotype monitoring growth curves (Fig. 2C). *brc142* -that had a

213 clear phenotype against several phages both in *E. coli* and *K. pneumoniae*- confirmed its broad
214 spectrum and host range, conferring resistance to Px5 at both MOI and to Px4 at low MOI ;
215 contrarily, *brcN* and *brcWGS21*, that had only shown low resistance against a handful of phages in
216 *E. coli*, conferred very high resistance against phage Px4 and Vs1 in *P. aeruginosa*. Altogether, our
217 data proves that BRiCs are active in different host species. Although some have a narrow host
218 range, others, like *brc142* conferred resistance in the three species against most phages tested.
219



220 **Fig. 2. Genetic Context, Recombination Frequency, and Phage Protection Profiles of Identified BRiCs in other**
221 **species. (A)** Genetic context of BRiCs as found in databases, highlighting their association with integron

222 integrases (*intI1* or *intI2*, in blue shades). BRiCs are found in different host species. Each BRiC is annotated with its respective
223 identifier (e.g., 59, 128A/B, 135A/B), along with known associated genes such as resistance genes (e.g., *blaIMP*, *aacA4*,
224 *catB6*). **(B)** Recombination frequency of the *attC* sites of the identified BRiCs. The recombination frequency was
225 measured for the bottom (green bars) and top (red bars) strands of the *attC* sites using a suicide conjugation assay. Bars
226 represent the mean of at least 3 biological replicates. Error bars correspond to the standard error of the mean. **(C)**
227 Heatmap showing the protection profiles of BRiCs against phage infection in different host species, including *K.*
228 *pneumoniae* (KP5) and *P. aeruginosa* (PAO1) against a panel of cognate phages (F13, Vs1, Px4, Px5). **(D)** Images of
229 transformant colonies of PAO1 showing abnormal morphologies.

230

231 BRiCs protect against prophage activation.

232 Conflicts between defense systems and MGEs can limit their spread through HGT. Mobile
233 integrons can reach new hosts through conjugation, so we asked if BRiCs could interfere with the
234 activation of existing prophages, protecting the host at the cell and/or the population level. To test
235 this, we introduced all BRiCs in lysogens of *E. coli* 594 with either HK544 or Φ80 prophages in
236 their genomes. We induced prophage activation with mitomycin and quantitated the phage titer
237 after 6 hours. *brc128*, *brc135* and *brc142* showed mild to strong defense against the activation of
238 HK544, with 20 to 1.000 fold decreases in titers. Brc59 completely abolished the production of
239 HK544 virions, showing $>10^7$ fold protection (Fig. 3A). Resistance against Φ80 activation was
240 generally very mild, with only *brcN*, *brc167*, and *brc233* producing low but statistically significant
241 resistance levels. Interestingly, there is not a clear correlation between defense against the free
242 phage (Fig. 1B and 1D) and prophage activation. Certain systems, like *brc135* and *brc142* confer
243 resistance against both forms of a phage HK544; while others, like *brc128*, *brc167.2* and *brc217*
244 only conferred resistance against one. These results show that mobile integrons containing BRiCs

245 can interfere with prophage activation, highlighting the potential protective effect at the community
246 level, and the complex interplay between MGEs.

247

248 ***brc128* does not have anti-plasmid activity.**

249 Brc128B shows strong structural similarities with DdmC (Fig. 3B), a Lamassu system with
250 anti-plasmid activity in *Vibrio cholerae* (50). To explore if Brc128AB has anti-plasmid activity we
251 measured the stability of pMBA (a p15A replicon) in the presence of *brc128* and *ddmABC*. After
252 ca. 20 generations in the absence of selective pressure, pMBA was present in >97% of cells
253 expressing Brc128AB, while only in 19% of those expressing DdmABC (Fig. 3C). We extended
254 this study to KP5 whose three natural plasmids are distinguishable for their resistance profile
255 (tetracycline, ertapenem or cefotaxime) and again found no effect of *brc128* in plasmid stability
256 (Fig. S5). This shows that, despite their structural similarities, Brc128AB does not have the anti-
257 p15A plasmid activity of DdmABC and suggests it might not be an anti-plasmid system.

258

259 **Deva interferes with genome injection.**

260 Deva (*brcWGS21*) confers a 10-fold protection and a small plaque phenotype against T7.
261 To provide insight on Deva's mechanism of action we evolved T7 to evade its activity. After two
262 rounds of infection, we retrieved phages producing large plaques and similar titers in the presence
263 and absence of Deva (Fig. 3D). Population sequencing with long reads revealed mutations in the
264 genes encoding gp0.7, gp12 and gp14 (Fig. 3E). gp0.7 is a kinase that phosphorylates the host RNA
265 polymerase to produce a transcriptional shutoff. The mutation in gp0.7 is pervasive: it is present in
266 all mutant combinations, and is the only one found alone, suggesting that it is the first one to appear
267 and that it plays a primary role in evading Deva. gp12, and gp14 are structural genes encoding tail
268 and internal virion protein B respectively. The latter is ejected into the cell during DNA injection.
269 Hence, mutations in gp12 and gp14 suggest that Deva interferes specifically with genome injection.
270 This is in accordance with its probable localization in the cell membrane (see transmembrane
271 domain and quaternary structure prediction in Fig. 1E and F).

272

273 **Functional analysis of Cosus**

274 Cosus (*brc24*) provides complete resistance against T7, with no detectable plaques in spot
275 assays. To investigate it further, we tried to evolve phages to evade its activity, but were unable to
276 retrieve plaques even when infecting with high phage titers (10^8 plaque forming units (pfus)). In
277 the absence of plaques, we tested if T7 mutants that evolved to escape other anti-phage mechanisms
278 could evade Cosus. We tested phages with K3Q and D131 substitutions in gp2.5 (ssDNA binding
279 protein (SSB)) (Fig. 3E) allowing to avoid retron-mediated defense (51) but saw no crossed evasion
280 between systems. We changed our approach to altering Cosus and generated 11 mutants in residues
281 predicted to be important in the activity of its RNA-binding PIN12 domain (52). Mutations T12A,
282 D14A and D96A led to a strong ($>10^5$ -fold) decrease in resistance to only 100-fold protection, and
283 a small plaque phenotype, supporting the correct identification of the PIN12 domain (Fig. 3F).
284 Retron evaders did not show enhanced activity in any Brc mutant, suggesting that Cosus does not
285 target T7 SSB. We then evolved T7 to evade Brc_{D14A} and obtained a 5-fold increase in pfu count
286 and plaques with an intermediate size. The evolved phage could also evade Brc_{T12A}, but not
287 Brc_{D96A} nor wild type Brc24. Genome sequencing revealed exclusively a non-synonymous
288 mutation in the tail protein gp12 (Fig. 3E), pointing to interference with genome injection too.
289 Taken together, our data hints at a potential dual activity of Cosus, that could explain the difficulties
290 to evolve T7 evaders.

291

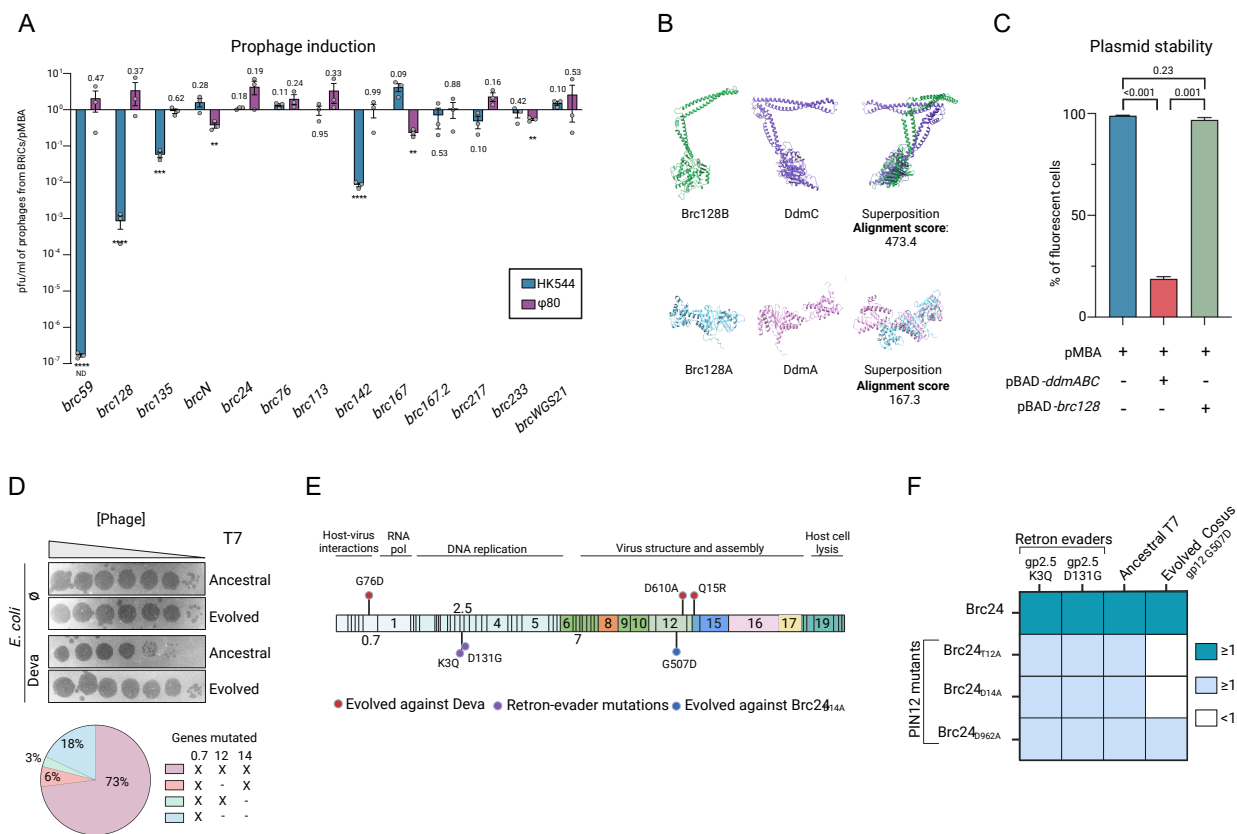


Fig. 3. Prophage Induction, Structural Alignment, and Impact of *brc128* on Plasmid Stability. (A) Prophage induction measured as the ratio of plaque-forming units per millilitre (pfu/ml) in the presence of pMBA containing BRICs over the empty pMBA. ND: not detected (Limits of detection plotted). One sample *t* and Wilcoxon test; *P* values are shown when possible; **<0.01; ***<0.001; ****<0.0001. (B) Structural alignment and superposition of Brc128A and Brc128B proteins with DdmA and DdmC. Alignment scores indicate the degree of structural similarity. (C) Plasmid stability assays in *E. coli*. Percentage of fluorescent cells is used to measure the stability of pMBA. Bars represent the mean of at least 3 biological replicates. Error bars correspond to the standard error of the mean. *P* values of unpaired *t*-tests are shown. (D) Plaque assays showing T7 evasion from Deva. Mutation distribution in the population. (E) Location of mutations in the genome of T7. (F) Resistance profile of PIN12 mutants of Cosus and defense-evading phages.

BRICs entail different fitness effects that vary across species.

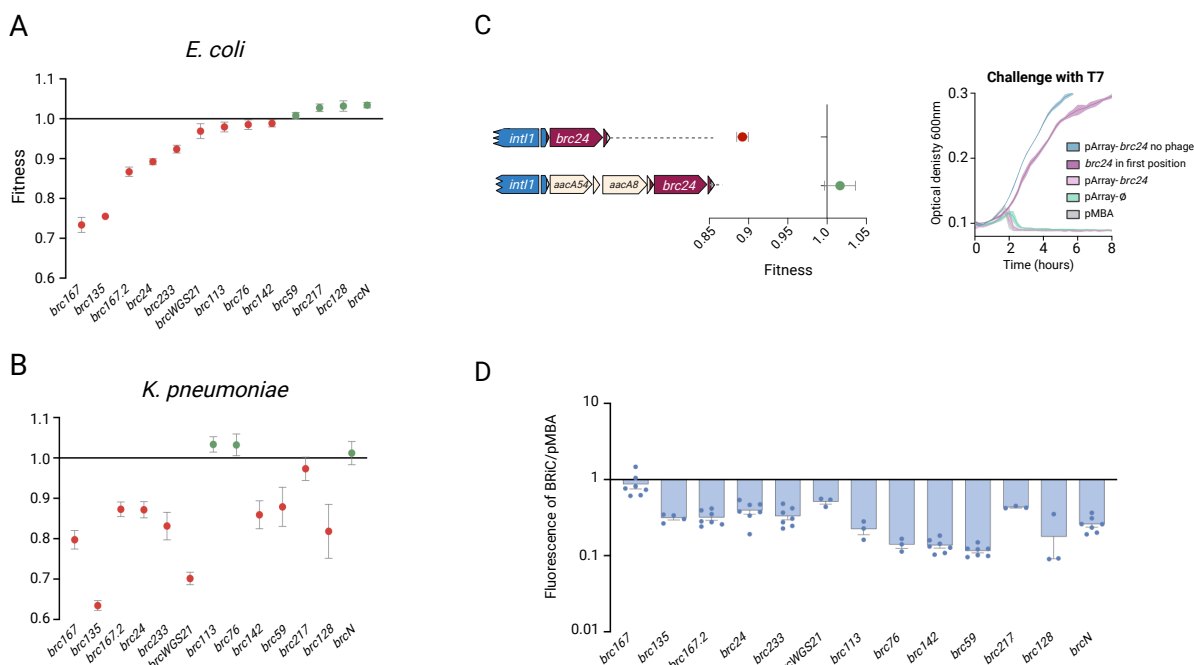
How defense systems affect the fitness of the host has important implications in their accumulation in genomes and their spread between species. Integrons are low-cost platforms that can modulate the expression of genes in the array by shuffling positions (20, 21, 53). To determine the cost of BRICs, we performed competition assays in both *E. coli* and *K. pneumoniae* (Fig. 4). Our results showed a broad distribution of fitness effects among BRICs, ranging from large costs (ca. 40%) to mildly positive (up to 3%) suggesting that acquisition of certain systems can be costless (Fig. 4A). It is of note that we have used a strong version of the *Pc* promoter, and that the cost of cassettes is probably lower in MIs with weaker *Pcs*. Comparison between species shows that fitness effects are not conserved between genetic backgrounds. For instance, *brcWGS21* entailed a small cost (ca. 7%) in *E. coli* but was very costly (ca. 30%) in *K. pneumoniae* (Fig. 4B). Only a few cassettes, like *brcN* showed very similar cost in both species. The lack of cost of BRICs in certain genetic backgrounds, and the differences in fitness effects across backgrounds can be of

317 importance in the accumulation of cassettes and their preferential distribution of BRiCs among
318 species.

319

320 **Integrons modulate the cost of BRiCs.**

321 In integrons, expression of cassettes depends on their proximity to the *Pc* and the polar
322 effects that cassettes upstream can exert (21). Because the expression and fitness cost of a gene
323 generally correlate, we hypothesize that integrons can modulate the cost of BRiCs. To test this, we
324 measured the cost of *brc24* in first and third position (as it is found in the databases (Fig. 2A))
325 downstream of cassettes with strong polar effects (*aacA54* and *aacA8*) (21). Cost of *brc24*
326 decreased from 11% in first position, to no significant cost in third (Fig. 4C). This was indeed due
327 to the strong repression of its expression, since phage infection experiments showed pArray-*brc24*
328 did not protect against T7 infection. Hence, costly BRiCs can be carried by mobile integrons at no
329 cost to be later reshuffled into first position, providing phage resistance on demand (23). We also
330 measured the polar effects exerted by BRiCs on downstream cassettes (Fig. 4D), showing that they
331 too participate in the modulation of function and cost of downstream genes in the array (21).



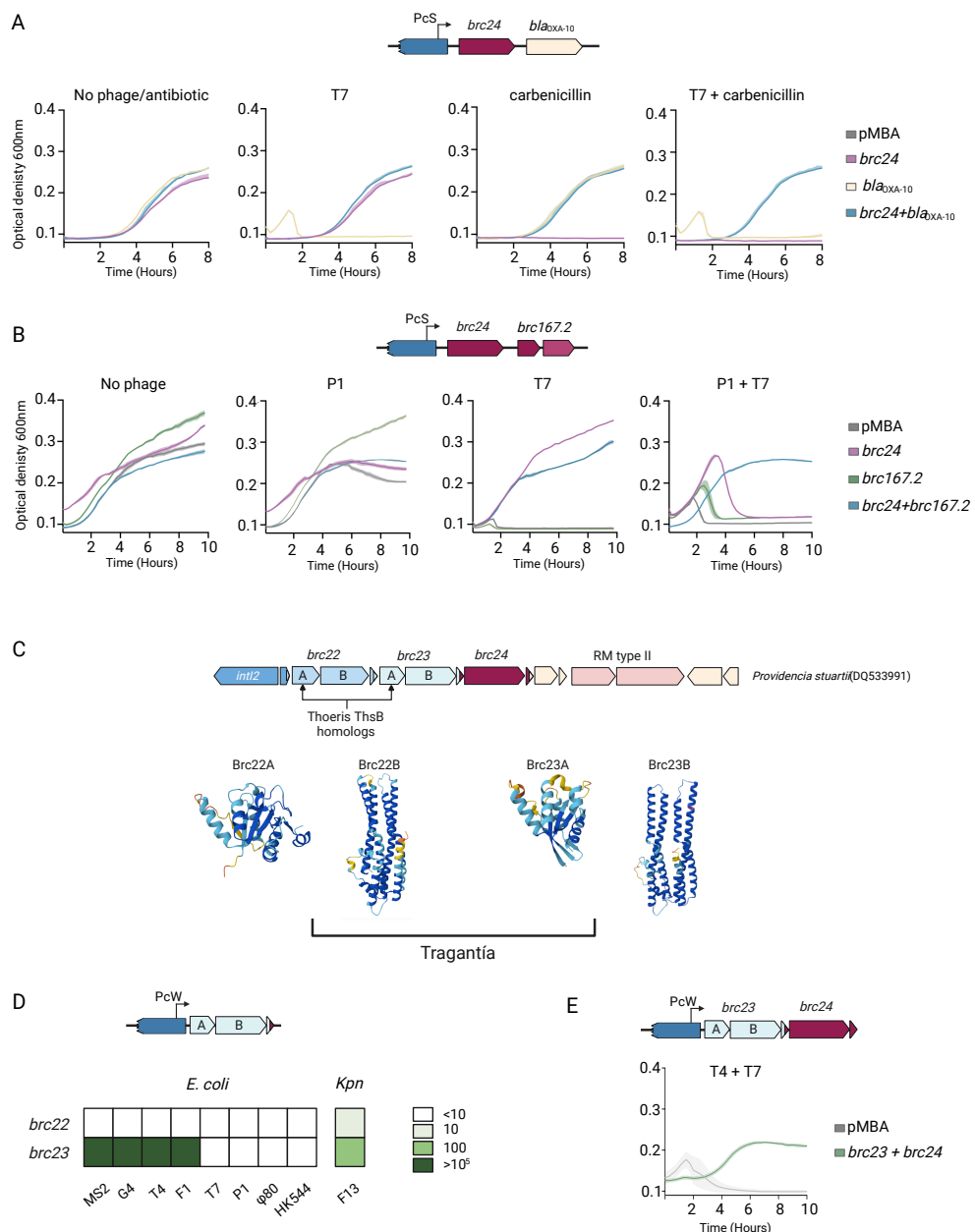
332
333 **Fig. 4. Fitness Effects of BRiCs.** Fitness effects of BRiCs in (A) *E. coli* and (B) *K. pneumoniae*. Red circles represent
334 fitness values below 1 (cost), while green circles indicate fitness values above 1 (gain). Fitness effects vary in sign and
335 magnitude and are not conserved among genetic backgrounds. (C) Modulation of fitness cost and function by integron
336 position. The graph shows the fitness effect of *brc24* in first position (competing pMBA vs pMBA-*brc24*) and third
337 position (pArrayØ vs. pArray-*brc24*). The fitness cost imposed by the BRiC is reduced in third position behind cassettes
338 with strong polar effects. The cost is related to the function of the BRiC since pArray-*brc24* does not confer resistance
339 to T7. (D) Polar effects of BRiCs. All cassettes except *brc167* exert polar effects on downstream cassettes, limiting
340 their expression. All assays have been performed at least three times. Error bars represent the standard error of the
341 mean.

342

343 **Mobile Integrons can accumulate resistance to phages and antibiotics.**

344 Being recombination platforms capturing cassettes with adaptive value, integrons could
345 potentially combine BRiCs and ARCs to provide multi-phage and drug resistance. To test this, we
346 combined *brc24* ($T7^R$) with the *blaOXA-10* β -lactamase and confirmed that it conferred high T7 and

347 carbenicillin resistance separately and simultaneously (Fig. 5A). We then built an array combining
348 *brc24* and *brc167.2* (P1^R) (Fig. 5B) and showed it conferred resistance against both phages,
349 confirming the additivity of BRiC and ARC phenotypes. Because MIs are enriched in AMR genes,
350 natural examples of arrays combining ARCs and BRiCs are abundant (see Fig. 2A for examples).
351 *gcus* are less abundant, so we did not find co-occurrence of BRiCs within an array. Nevertheless,
352 having found here a variety of two-gene BRiCs, the genetic environment of *brc24* (preceded by
353 two such cassettes) was re-evaluated. An update of DefenseFinder (June 2024) found homologs of
354 sensor protein ThsB from the Thoeris system in the first ORF of both cassettes (*gcu23* and *gcu24*),
355 and a type II restriction modification system downstream the last cassette (Fig. 5C). *gcu23* and
356 *gcu24* share 50% bp identity, and a remarkably conserved predicted structure of their two ORFs.
357 While Brc22A and Brc23A are predicted homologs of Thoeris ThsB, Brc22B and Brc23B are
358 shorter than ThsA (300 vs. 500 aminoacids), show a very low protein identity (ca. 13%) and a very
359 different predicted fold, suggesting that these genes are not homologs. The predicted structure of
360 these proteins is instead similar to Deva (*brcWGS21*) (Fig. 1F). Both *gcu22* and *gcu23* were present
361 in our collection, but not selected in our screenings because *gcu22* did not confer resistance to any
362 phage, and *gcu23* showed inconsistent results and was discarded. We found that the cassette in our
363 stock strain was frequently interrupted by the insertion of IS1, which explained the inconsistency.
364 We interpreted this as a sign of high fitness cost, so we cloned both cassettes under a weak Pc
365 (PcW) and tested them against the panel of phages in *E. coli* and *K. pneumoniae*. *gcu22* conferred
366 low levels of resistance exclusively against phage F13 in *K. pneumoniae*, while *gcu23* had a broader
367 defense profile, including very high resistance levels against G4, MS2, F1 and T4) (Fig. 5D). We
368 hence redefined both cassettes as BRiCs (*brc22* and *brc23*) and, given the apparent hybrid genetic
369 structure mentioned before, we consider this a novel system that we have called Tragantía (a deity
370 with the upper body of a woman and the lower body of a snake). Finally, to show that this integron
371 acts as a natural defense island we built an array containing *brc23* and *brc24* (the only ones with
372 distinguishable phenotypes) and showed that it confers multi-phage resistance against T7 and T4
373 (Fig. 5E). Hence MIs naturally act as mobile defense islands that already circulate among clinical
374 isolates (54).



375

376 **Fig. 5. Additivity of Phage and Antibiotic Resistance Phenotypes in Multi-Cassette Arrays.** Growth curves
377 (OD₆₀₀) of *E. coli* strains containing (A) pMBA, *brc24* and *blaOXA-10* independently, and combined in an array in the
378 absence of phage or antibiotic, and challenged with phage T7, carbenicillin, and a combination of both. The combined
379 array confers resistance to phage and antibiotics simultaneously, and (B) pMBA, *brc24* and *brc167.2* independently,
380 and combined in an array; either with no phage, or challenged with phage P1, phage T7, and a combination of both.
381 (C) Genetic background of *brc24*, *brc22* and *brc23* contain homologs to ThsB from Thoeris that confer resistance
382 against phages from *E. coli* and *K. pneumoniae* (Kpn). *brc23* and *brc24* can confer multiphage resistance when in the
383 same array. Growth curves are represented as the mean of three independent replicates. The standard error of the mean
384 is represented as a lighter colour shade.

385

386

387

388

389 **Defense systems in BRiCs are found outside integrons.**

390 Integron cassettes are exchanged between integrons cohabiting the same cell. MIs can scan
391 sedentary chromosomal integrons (SCIs) and bring to clinical settings adaptive functions evolved
392 elsewhere in the biosphere (55). This suggests that BRiCs are likely found in SCIs. In an article in
393 this issue Darracq *et al.* provide evidence that the Superintegron in *V. cholerae* contains indeed a
394 variety of BRiCs, that are different from the ones described here (56). We hence sought to
395 investigate the potential origin and distribution of our defense systems. We have searched for
396 homologs in databases and examined their genetic context (Fig. S6). Certain systems show a broad
397 distribution among integrons, like *brcN*, that is found in MIs and SCIs of the *Pseudomonadaceae*
398 family (Fig. 6A), consistent with its resistance phenotype in *P. aeruginosa*. Homologs of Brc24
399 (Cosus) are found as BRiCs in integron arrays in *Marinobacter salexigens* (Fig. 6B). They are also
400 found in genomes of *Vibrio* species, outside their SCIs but with a conserved *attC* site, suggesting
401 that this could be a *bona fide* cassette integrated into an *attG* site in the chromosome (57).
402 Interestingly, BrcN and Brc24 homologs were also found isolated without recognizable *attC* sites
403 in the genomes of *Kangiella japonica* and *Escherichia marmotae* (Fig. 6C and Fig. S7). The
404 Tragantía system in *brc22* has homologs often found in the vicinity of other PDSs. We found one
405 in the chromosome of *Marinobacter sp.* CuT6 (Fig. 6D). This isolate has a complete integron and
406 CALIN (cassette array lacking an integrase), but the Tragantía homolog was encoded elsewhere,
407 within a small defense island together with homologs of Thoeris and Gao (58). This system shows
408 95% amino acid identity with Brc22A and B, but has a pseudo *attC* site in which extrahelical bases
409 are located at both sides of the stem, and a mismatch is found in the conserved crossover point.
410 This likely makes it non-recombinogenic (Fig. S8). While this does not seem to be a *bona fide*
411 integron cassette (and it is not recognised by IntegronFinder), it is strikingly close (only a few
412 mutations away) from a canonical one. Altogether, the high plasticity in the genetic context of these
413 systems and their *attC* sites suggest a dynamic recruitment of PDSs from defense islands to
414 integrons.

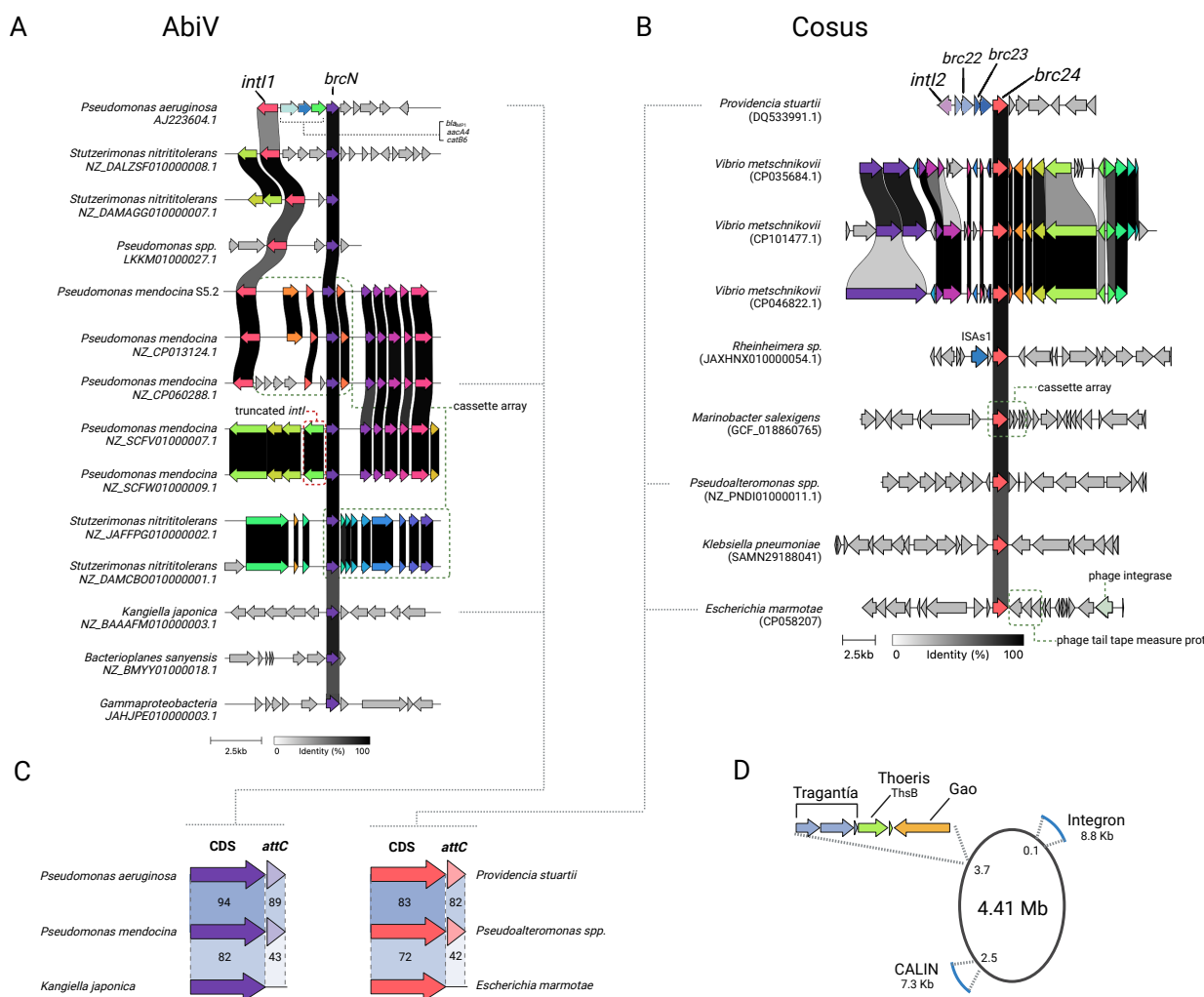


Fig. 6. Genetic context of BRiC homologs. Analysis of the genetic environments of AbiV (*brcN*) (A) and Cosus (*brc24*) (B) showing their distribution in mobile and sedentary chromosomal integrons of different species. Integron integrases and arrays are marked where recognised. Some homologs to BRiCs are also found outside integrons, and, despite a good sequence conservation in the coding region, they lack *attC* sites (C). A Tragantia system, homolog of *brc22*, is found within a small defense island in the chromosome of *Marinobacter* spp. and contains a pseudo *attC* site. This isolate contains an SCI and a CALIN (D).

DISCUSSION

In this work we show that mobile integrons act as highly-mobile, low-cost defense islands. We have successfully identified 47 new BRiCs experimentally, and have characterized in depth 15 of them. BRiCs displayed different specificities conferring narrow to broad immunity in our assays.

Our work is not free from limitations. First, while our screening successfully retrieved 45 BRiCs in the *gcu* collection, it is likely that others went undetected given the variety of bacterial species in which *gcu*s have been found. Indeed, it is probable that other PDSs would be discovered if we could test them in other bacterial species against their phages. This rationale could also apply to our plasmid stability assays, where testing more plasmids might reveal an anti-plasmid activity in Brc128. Nevertheless, despite the structural similarities, Brc128B and DdmC belong to different types of Lamassu systems and Brc128B does not contain the Walker B motif found in DdmC.

434 Hence, we cannot rule out intrinsic functional differences between both systems. In this sense, the
435 lack of anti-plasmid activity in Brc128AB might have been selected for in conjugative plasmids
436 navigating an environment with high antibiotic pressure. Additionally, detection algorithms are
437 being constantly improved, so prediction of BRiCs in *gcus* will likely yield more hits at the time
438 this work is published.

439 This study reshapes our perception of integrons. The presence of PDSs and AMR genes,
440 proposes that integrons are protection elements against a large breadth of environmental insults.
441 Our data also highlights for the first time the crosstalk between integrons and genomes with a
442 multitude of examples of BRiCs closely related homologs outside integrons. The study of BRiCs
443 might help reveal the genesis of cassettes, a long-standing question in the field. Being part of an
444 integron has a profound impact in the biology and ecology of PDSs and of bacterial defense
445 strategies. Encoded in BRiCs, PDSs become extremely mobile genetic elements that can be
446 combined to confer multi-phage or phage-drug resistance and shuffled to modulate their cost. An
447 extreme case of cost modulation is the Superintegron of *Vibrio cholerae* a large structure carried at
448 no measurable cost (59) that contains several BRiCs, as shown by Darracq *et al.* in a paper in this
449 issue. Additionally, their findings highlight that SCIs are extensive repositories of BRiCs for MIs.

450 Phage therapy is an old approach with renewed interest in the light of the AMR crisis (60,
451 61). It allows for personalized treatments against multidrug resistant bacteria, with encouraging
452 outcomes against multidrug resistant isolates. Mobile integrons have significantly contributed to
453 the AMR crisis bringing to our hospitals a plethora of ARCs from the genomes of environmental
454 bacteria. Being shed to the environment at extremely high quantities (10^{23} per day) (62), MIs
455 connect the genomes of pathogenic and environmental bacteria (63). The rampant movement of
456 MIs among clinically-relevant bacteria ensures a rapid dissemination of any novel adaptive
457 function in our hospitals. We have shown that BRiCs can confer resistance in 3 of the 5 Gram
458 negative species of the ESKAPEE group of highly resistant and dangerous pathogens: the kind of
459 bacteria aimed by phage therapy assays. This strongly suggests that the spread of BRiCs among
460 them will be quick if selective pressure with phages becomes commonplace. This has implications
461 in what are today considered as exploitable trade-offs in phage therapy. For instance, it is known
462 that many *K. pneumoniae* phages bind the bacterial capsule and that resistant clones can easily arise
463 through capsule loss, albeit at the cost of becoming non-virulent (64). Also, in some cases becoming
464 resistant to phage infection through mutations comes at the cost of losing antibiotic resistance (65,
465 66). The acquisition of plasmids containing integrons with BRiCs can abrogate the exploitability
466 of such trade-offs, rendering virulence and antibiotic resistance perfectly compatible with phage
467 resistance. Altogether, our results highlight that the role of integrons in phage defense can be critical
468 for the advent of phage therapy.

469 The role of MIs in phage resistance showcases the interplay between MGEs. Many of the
470 BRiCs described here confer resistance against phages that target the conjugative pilus of *E. coli*
471 IJ1862. Hence, BRiCs can be beneficial for conjugative plasmids and foster HGT by alleviating
472 the trade-off between acquiring adaptive plasmids and becoming susceptible to a large variety of
473 phages. Nevertheless, the fact that we couldn't introduce many systems in *P. aeruginosa* (even
474 under a P_cW) suggests that some BRiCs can also act as barriers to HGT.

475 Altogether, we show that MIs can act as mobile and low-cost phage defense islands. Being
476 able to exchange BRiCs between plasmids and to move across genetic backgrounds, MIs are likely
477 important players in the complex interactions between mobile genetic elements.

478

479 **References:**

- 480 1. Antimicrobial Resistance Collaborators, Global burden of bacterial antimicrobial
481 resistance in 2019: a systematic analysis. *Lancet* **399**, 629–655 (2022).
- 482 2. F. d'Herelle, Bacteriophage as a Treatment in Acute Medical and Surgical Infections. *Bull
483 N Y Acad Med* **7**, 329–48 (1931).
- 484 3. G. F. Hatfull, R. M. Dedrick, R. T. Schooley, Phage Therapy for Antibiotic-Resistant
485 Bacterial Infections. *Annu Rev Med* **73**, 197–211 (2022).
- 486 4. K. E. Kortright, B. K. Chan, J. L. Koff, P. E. Turner, Phage Therapy: A Renewed Approach
487 to Combat Antibiotic-Resistant Bacteria. *Cell Host Microbe* **25**, 219–232 (2019).
- 488 5. S. J. Labrie, J. E. Samson, S. Moineau, Bacteriophage resistance mechanisms. *Nat Rev
489 Microbiol* **8**, 317–27 (2010).
- 490 6. J. T. Rostøl, L. Marraffini, (Ph)ighting Phages: How Bacteria Resist Their Parasites. *Cell
491 Host Microbe* **25**, 184–194 (2019).
- 492 7. A. Bernheim, R. Sorek, The pan-immune system of bacteria: antiviral defence as a
493 community resource. *Nat Rev Microbiol* **18**, 113–119 (2020).
- 494 8. C. N. Vassallo, C. R. Doering, M. L. Littlehale, G. I. C. Teodoro, M. T. Laub, A functional
495 selection reveals previously undetected anti-phage defence systems in the *E. coli*
496 pan-genome. *Nat Microbiol* **7**, 1568–1579 (2022).
- 497 9. R. M. Dedrick, D. Jacobs-Sera, C. A. G. Bustamante, R. A. Garlena, T. N. Mavrich, W. H.
498 Pope, J. C. C. Reyes, D. A. Russell, T. Adair, R. Alvey, J. A. Bonilla, J. S. Bricker, B. R.
499 Brown, D. Byrnes, S. G. Cresawn, W. B. Davis, L. A. Dickson, N. P. Edgington, A. M.
500 Findley, U. Golebiewska, J. H. Grose, C. F. Hayes, L. E. Hughes, K. W. Hutchison, S.
501 Isern, A. A. Johnson, M. A. Kenna, K. K. Klyczek, C. M. Magee, S. F. Michael, S. D.
502 Molloy, M. T. Montgomery, J. Neitzel, S. T. Page, M. C. Pizzorno, M. K. Poxleitner, C. A.
503 Rinehart, C. J. Robinson, M. R. Rubin, J. N. Teyim, E. Vazquez, V. C. Ware, J.
504 Washington, G. F. Hatfull, Prophage-mediated defence against viral attack and viral
505 counter-defence. *Nat Microbiol* **2**, 16251 (2017).
- 506 10. A. Millman, S. Melamed, A. Leavitt, S. Doron, A. Bernheim, J. Hör, J. Garb, N. Bechon,
507 A. Brandis, A. Lopatina, G. Ofir, D. Hochhauser, A. Stokar-Avihail, N. Tal, S. Sharir, M.
508 Voichek, Z. Erez, J. L. M. Ferrer, D. Dar, A. Kacen, G. Amitai, R. Sorek, An expanded
509 arsenal of immune systems that protect bacteria from phages. *Cell Host Microbe* **30**, 1556–
510 1569.e5 (2022).
- 511 11. D. Hochhauser, A. Millman, R. Sorek, The defense island repertoire of the *Escherichia coli*
512 pan-genome. *PLoS Genet* **19**, e1010694 (2023).
- 513 12. K. S. Makarova, Y. I. Wolf, S. Snir, E. V. Koonin, Defense Islands in Bacterial and
514 Archaeal Genomes and Prediction of Novel Defense Systems. *J Bacteriol* **193**, 6039–6056
515 (2011).
- 516 13. T. M. Ghaly, M. R. Gillings, A. Penesyan, Q. Qi, V. Rajabal, S. G. Tetu, The Natural
517 History of Integrons. *Microorganisms* **9** (2021).
- 518 14. M. Labbate, R. J. Case, H. W. Stokes, “The Integron/Gene Cassette System: An Active
519 Player in Bacterial Adaptation” (2009; http://link.springer.com/10.1007/978-1-60327-853-9_6), pp. 103–125.
- 521 15. D. Mazel, Integrons: Agents of bacterial evolution. *Nat Rev Microbiol* **4**, 608–620 (2006).

522 16. G. D. Recchia, R. M. Hall, Gene cassettes: A new class of mobile element. *Microbiology (N Y)* **141**, 3015–3027 (1995).

523 17. S. R. Partridge, G. D. Recchia, C. Scaramuzzi, C. M. Collis, H. W. Stokes, R. M. Hall, Definition of the attI1 site of class 1 integrons. *Microbiology (N Y)* **146**, 2855–2864 (2000).

524 18. C. M. Collis, R. M. Hall, Expression of antibiotic resistance genes in the integrated cassettes of integrons. *Antimicrob Agents Chemother* **39**, 155–162 (1995).

525 19. O. Barraud, M. C. Ploy, Diversity of class 1 integron gene cassette rearrangements selected under antibiotic pressure. *J Bacteriol* **197**, 2171–2178 (2015).

526 20. C. Souque, J. A. Escudero, R. C. Maclean, Integron activity accelerates the evolution of antibiotic resistance. *Elife* **10**, 1–47 (2021).

527 21. A. Carvalho, A. Hipólito, F. T. da Roza, L. García-, E. Vergara, A. Buendía, T. García-Seco, A. Escudero, The expression of integron arrays is shaped by the translation rate of cassettes. doi: 10.1101/2024.03.26.586746.

528 22. É. Guerin, G. Cambray, N. Sanchez-Alberola, S. Campoy, I. Erill, S. Da Re, B. Gonzalez-Zorn, J. Barbé, M.-C. Ploy, D. Mazel, The SOS Response Controls Integron Recombination. *Science (1979)* **324**, 1034–1034 (2009).

529 23. J. A. Escudero, C. Loot, A. Nivina, D. Mazel, The Integron: Adaptation On Demand. *Mobile DNA III*, 139–161 (2015).

530 24. S. R. Partridge, S. M. Kwong, N. Firth, S. O. Jensen, Mobile Genetic Elements Associated with Antimicrobial Resistance. *Clin Microbiol Rev* **31** (2018).

531 25. H. W. Stokes, R. M. Hall, A novel family of potentially mobile DNA elements encoding site-specific gene-integration functions: integrons. *Mol Microbiol* **3**, 1669–1683 (1989).

532 26. S. Domingues, G. J. da Silva, K. M. Nielsen, Integrons: Vehicles and pathways for horizontal dissemination in bacteria. *Mob Genet Elements* **2**, 211–223 (2012).

533 27. M. Kaushik, S. Kumar, R. K. Kapoor, J. S. Virdi, P. Gulati, Integrons in Enterobacteriaceae : diversity, distribution and epidemiology. *Int J Antimicrob Agents* **51**, 167–176 (2018).

534 28. A. Hipólito, L. García-Pastor, E. Vergara, T. Jové, J. A. Escudero, Profile and resistance levels of 136 integron resistance genes. *npj Antimicrobials and Resistance* **1**, 13 (2023).

535 29. S. R. Partridge, G. Tsafnat, E. Coiera, J. R. Iredell, Gene cassettes and cassette arrays in mobile resistance integrons. *FEMS Microbiol Rev* **33**, 757–784 (2009).

536 30. A. Hipólito, L. García-Pastor, P. Blanco, F. Trigo da Roza, N. Kieffer, E. Vergara, T. Jové, J. Álvarez, J. A. Escudero, The expression of aminoglycoside resistance genes in integron cassettes is not controlled by riboswitches. *Nucleic Acids Res*, doi: 10.1093/nar/gkac662 (2022).

537 31. A. Moura, M. Soares, C. Pereira, N. Leitão, I. Henriques, A. Correia, INTEGRALL: A database and search engine for integrons, integrases and gene cassettes. *Bioinformatics* **25**, 1096–1098 (2009).

538 32. F. Tesson, A. Hervé, E. Mordret, M. Touchon, C. d’Humières, J. Cury, A. Bernheim, Systematic and quantitative view of the antiviral arsenal of prokaryotes. *Nat Commun* **13**, 2561 (2022).

564 33. L. J. Payne, S. Meaden, M. R. Mestre, C. Palmer, N. Toro, P. C. Fineran, S. A. Jackson,
565 PADLOC: a web server for the identification of antiviral defence systems in microbial
566 genomes. *Nucleic Acids Res* **50**, W541–W550 (2022).

567 34. F. Rousset, F. Depardieu, S. Miele, J. Dowding, A.-L. Laval, E. Lieberman, D. Garry, E. P.
568 C. Rocha, A. Bernheim, D. Bikard, Phages and their satellites encode hotspots of antiviral
569 systems. *Cell Host Microbe* **30**, 740-753.e5 (2022).

570 35. B. Duncan-Lowey, P. J. Kranzusch, CBASS phage defense and evolution of antiviral
571 nucleotide signaling. *Curr Opin Immunol* **74**, 156–163 (2022).

572 36. B. Duncan-Lowey, N. K. McNamara-Bordewick, N. Tal, R. Sorek, P. J. Kranzusch,
573 Effector-mediated membrane disruption controls cell death in CBASS antiphage defense.
574 *Mol Cell* **81**, 5039-5051.e5 (2021).

575 37. J. Haaber, S. Moineau, L.-C. Fortier, K. Hammer, AbiV, a novel antiphage abortive
576 infection mechanism on the chromosome of *Lactococcus lactis* subsp. *cremoris* MG1363.
577 *Appl Environ Microbiol* **74**, 6528–37 (2008).

578 38. J. J. Bull, M. R. Badgett, R. Springman, I. J. Molineux, Genome properties and the limits
579 of adaptation in bacteriophages. *Evolution (N Y)* **58**, 692 (2004).

580 39. N. Quinones-Olvera, S. V. Owen, L. M. McCully, M. G. Marin, E. A. Rand, A. C. Fan, O.
581 J. Martins Dosumu, K. Paul, C. E. Sanchez Castaño, R. Petherbridge, J. S. Paull, M.
582 Baym, Diverse and abundant phages exploit conjugative plasmids. *Nat Commun* **15**
583 (2024).

584 40. S. Wang, S. Kuang, H. Song, E. Sun, M. Li, Y. Liu, Z. Xia, X. Zhang, X. Wang, J. Han, V.
585 B. Rao, T. Zou, C. Tan, P. Tao, The role of TIR domain-containing proteins in bacterial
586 defense against phages. *Nat Commun* **15**, 7384 (2024).

587 41. A. Kelly, T. J. Arrowsmith, S. C. Went, T. R. Blower, Toxin–antitoxin systems as mediators
588 of phage defence and the implications for abortive infection. *Curr Opin Microbiol* **73**,
589 102293 (2023).

590 42. D. Matelska, K. Steczkiewicz, K. Ginalski, Comprehensive classification of the PIN
591 domain-like superfamily. *Nucleic Acids Res* **45**, 6995–7020 (2017).

592 43. C. D. Boyd, T. J. Smith, S. El-Kirat-Chatel, P. D. Newell, Y. F. Dufrêne, G. A. O’Toole,
593 Structural Features of the *Pseudomonas fluorescens* Biofilm Adhesin LapA Required for
594 LapG-Dependent Cleavage, Biofilm Formation, and Cell Surface Localization. *J Bacteriol*
595 **196**, 2775–2788 (2014).

596 44. B. Néron, E. Littner, M. Haudiquet, A. Perrin, J. Cury, E. P. C. Rocha, IntegronFinder 2.0:
597 Identification and Analysis of Integrons across Bacteria, with a Focus on Antibiotic
598 Resistance in *Klebsiella*. *Microorganisms* **10** (2022).

599 45. C. Loot, M. Ducas-Galand, J. A. Escudero, M. Bouvier, D. Mazel, Replicative resolution
600 of integron cassette insertion. *Nucleic Acids Res* **40**, 8361–8370 (2012).

601 46. M. Bouvier, M. Ducas-Galand, C. Loot, D. Bikard, D. Mazel, Structural features of single-
602 stranded integron cassette attC sites and their role in strand selection. *PLoS Genet* **5**
603 (2009).

604 47. A. Nivina, J. A. Escudero, C. Vit, D. Mazel, C. Loot, Efficiency of integron cassette
605 insertion in correct orientation is ensured by the interplay of the three unpaired features of
606 attC recombination sites. *Nucleic Acids Res* **44**, 7792–7803 (2016).

607 48. D. MacDonald, G. Demarre, M. Bouvier, D. Mazel, D. N. Gopaul, Structural basis for
608 broad DNA-specificity in integron recombination. *Nature* **440**, 1157–1162 (2006).

609 49. P. Blanco, A. Hipólito, L. García-Pastor, F. Trigo Da Roza, L. Toribio-Celestino, A. C.
610 Ortega, E. Vergara, Á. S. Millán, J. A. Escudero, Identification of Promoter Activity in
611 Gene-Less Cassettes from Vibrionaceae Superintegrons. *Nucleic Acids Research*. *In press*,
612 doi: 10.1101/2023.11.21.568050 (2023).

613 50. M. Jaskólska, D. W. Adams, M. Blokesch, Two defence systems eliminate plasmids from
614 seventh pandemic *Vibrio cholerae*. *Nature* **604**, 323–329 (2022).

615 51. A. Fillol-Salom, J. T. Rostøl, A. D. Ojiogu, J. Chen, G. Douce, S. Humphrey, J. R.
616 Penadés, Bacteriophages benefit from mobilizing pathogenicity islands encoding immune
617 systems against competitors. *Cell* **185**, 3248-3262.e20 (2022).

618 52. M. Senissar, M. C. Manav, D. E. Brodersen, Structural conservation of the PIN domain
619 active site across all domains of life. *Protein Science* **26**, 1474–1492 (2017).

620 53. Y. Lacotte, M.-C. Ploy, S. Raherison, Class 1 integrons are low-cost structures in
621 *Escherichia coli*. *ISME J* **11**, 1535–1544 (2017).

622 54. R. S. Barlow, K. S. Gobius, Diverse class 2 integrons in bacteria from beef cattle sources.
623 *Journal of Antimicrobial Chemotherapy* **58**, 1133–1138 (2006).

624 55. D. A. Rowe-Magnus, A. M. Guerout, D. Mazel, Bacterial resistance evolution by
625 recruitment of super-integron gene cassettes. *Mol Microbiol* **43**, 1657–1669 (2002).

626 56. B. Darracq, E. Littner, M. Brunie, J. Bos, P.-A. Kaminski, F. Depardieu, W. Slesak, K.
627 Debatisse, M. Touchon, A. Bernheim, D. Bikard, F. Le Roux, D. Mazel, E. P. C. Rocha, C.
628 Loot, Sedentary chromosomal integrons as biobanks of bacterial anti-phage defence
629 systems. doi: 10.1101/2024.07.02.601686.

630 57. C. Loot, G. A. Millot, E. Richard, E. Littner, C. Vit, F. Lemoine, B. Néron, J. Cury, B.
631 Darracq, T. Niault, D. Lapaillerie, V. Parissi, E. P. C. Rocha, D. Mazel, Integron cassettes
632 integrate into bacterial genomes via widespread non-classical attG sites. *Nat Microbiol* **9**,
633 228–240 (2024).

634 58. L. Gao, H. Altae-Tran, F. Böhning, K. S. Makarova, M. Segel, J. L. Schmid-Burgk, J.
635 Koob, Y. I. Wolf, E. V. Koonin, F. Zhang, Diverse enzymatic activities mediate antiviral
636 immunity in prokaryotes. *Science (1979)* **369**, 1077–1084 (2020).

637 59. P. Blanco, F. Trigo da Roza, L. Toribio-Celestino, L. García-Pastor, N. Caselli, F. Ojeda, B.
638 Darracq, E. Vergara, Á. San, O. Skovgaard, D. Mazel, C. Loot, J. Antonio Escudero,
639 Chromosomal Integrons are Genetically and Functionally Isolated Units of Genomes 2 3.
640 doi: 10.1101/2023.11.17.567518.

641 60. M. Corbellino, N. Kieffer, M. Kutateladze, N. Balarjishvili, L. Leshkasheli, L.
642 Askilashvili, G. Tsertsvadze, S. G. Rimoldi, D. Nizharadze, N. Hoyle, L. Nadareishvili, S.
643 Antinori, C. Pagani, D. G. Scorza, A. L. L. Romanò, S. Ardizzone, P. Danelli, M. R.
644 Gismondo, M. Galli, P. Nordmann, L. Poirel, Eradication of a Multidrug-Resistant,
645 Carbapenemase-Producing *Klebsiella pneumoniae* Isolate Following Oral and Intra-rectal
646 Therapy With a Custom Made, Lytic Bacteriophage Preparation. *Clinical Infectious
647 Diseases* **70**, 1998–2001 (2020).

648 61. J.-P. Pirnay, S. Djebara, G. Steurs, J. Griselain, C. Cochez, S. De Soir, T. Glonti, A.
649 Spiessens, E. Vandenberghe, S. Green, J. Wagemans, C. Lood, E. Schrevens, N.

650 Chanishvili, M. Kutatladze, M. de Jode, P.-J. Ceyssens, J.-P. Draye, G. Verbeken, D. De
651 Vos, T. Rose, J. Onsea, B. Van Nieuwenhuyse, Bacteriophage Therapy Providers,
652 Bacteriophage Donors, P. Soentjens, R. Lavigne, M. Merabishvili, Personalized
653 bacteriophage therapy outcomes for 100 consecutive cases: a multicentre, multinational,
654 retrospective observational study. *Nat Microbiol* **9**, 1434–1453 (2024).

655 62. Y.-G. Zhu, M. Gillings, P. Simonet, D. Stekel, S. Banwart, J. Penuelas, Microbial mass
656 movements. *Science* (1979) **357**, 1099–1100 (2017).

657 63. M. Gillings, Y. Boucher, M. Labbate, A. Holmes, S. Krishnan, M. Holley, H. W. Stokes,
658 The evolution of class 1 integrons and the rise of antibiotic resistance. *J Bacteriol* **190**,
659 5095–5100 (2008).

660 64. L. Song, X. Yang, J. Huang, X. Zhu, G. Han, Y. Wan, Y. Xu, G. Luan, X. Jia, Phage
661 Selective Pressure Reduces Virulence of Hypervirulent *Klebsiella pneumoniae* Through
662 Mutation of the *wzc* Gene. *Front Microbiol* **12** (2021).

663 65. J. Fujiki, K. Nakamura, T. Nakamura, H. Iwano, Fitness Trade-Offs between Phage and
664 Antibiotic Sensitivity in Phage-Resistant Variants: Molecular Action and Insights into
665 Clinical Applications for Phage Therapy. *Int J Mol Sci* **24**, 15628 (2023).

666 66. B. K. Chan, M. Sistrom, J. E. Wertz, K. E. Kortright, D. Narayan, P. E. Turner, Phage
667 selection restores antibiotic sensitivity in MDR *Pseudomonas aeruginosa*. *Sci Rep* **6**, 26717
668 (2016).

669 67. N. Alqurainy, L. Miguel-Romero, J. Moura de Sousa, J. Chen, E. P. C. Rocha, A. Fillol-
670 Salom, J. R. Penadés, A widespread family of phage-inducible chromosomal islands only
671 steals bacteriophage tails to spread in nature. *Cell Host Microbe* **31**, 69-82.e5 (2023).

672 68. N. Bonilla, M. I. Rojas, G. Netto Flores Cruz, S.-H. Hung, F. Rohwer, J. J. Barr, Phage on
673 tap-a quick and efficient protocol for the preparation of bacteriophage laboratory stocks.
674 *PeerJ* **4**, e2261 (2016).

675 69. N. Ács, M. Gambino, L. Brøndsted, Bacteriophage Enumeration and Detection Methods.
676 *Front Microbiol* **11**, 594868 (2020).

677 70. F. Tesson, A. Hervé, E. Mordret, M. Touchon, C. d’Humières, J. Cury, A. Bernheim,
678 Systematic and quantitative view of the antiviral arsenal of prokaryotes. *Nat Commun* **13**,
679 2561 (2022).

680 71. M. van Kempen, S. S. Kim, C. Tumescheit, M. Mirdita, J. Lee, C. L. M. Gilchrist, J.
681 Söding, M. Steinegger, Fast and accurate protein structure search with Foldseek. *Nat
682 Biotechnol*, doi: 10.1038/s41587-023-01773-0 (2023).

683 72. M. Mirdita, K. Schütze, Y. Moriwaki, L. Heo, S. Ovchinnikov, M. Steinegger, ColabFold:
684 making protein folding accessible to all. *Nat Methods* **19**, 679–682 (2022).

685 73. J. Yang, Y. Zhang, Protein Structure and Function Prediction Using I-TASSER. *Curr
686 Protoc Bioinformatics* **52** (2015).

687 74. C. L. M. Gilchrist, Y.-H. Chooi, clinker & clustermap.js: automatic generation of gene
688 cluster comparison figures. *Bioinformatics* **37**, 2473–2475 (2021).

689 75. J. Jumper, R. Evans, A. Pritzel, T. Green, M. Figurnov, O. Ronneberger, K.
690 Tunyasuvunakool, R. Bates, A. Žídek, A. Potapenko, A. Bridgland, C. Meyer, S. A. A.
691 Kohl, A. J. Ballard, A. Cowie, B. Romera-Paredes, S. Nikolov, R. Jain, J. Adler, T. Back,
692 S. Petersen, D. Reiman, E. Clancy, M. Zielinski, M. Steinegger, M. Pacholska, T.

693 Berghammer, S. Bodenstein, D. Silver, O. Vinyals, A. W. Senior, K. Kavukcuoglu, P.
694 Kohli, D. Hassabis, Highly accurate protein structure prediction with AlphaFold. *Nature*
695 **596**, 583–589 (2021).

696 76. V. Bortolaia, R. S. Kaas, E. Ruppe, M. C. Roberts, S. Schwarz, V. Cattoir, A. Philippon, R.
697 L. Allesoe, A. R. Rebelo, A. F. Florensa, L. Fagelhauer, T. Chakraborty, B. Neumann, G.
698 Werner, J. K. Bender, K. Stingl, M. Nguyen, J. Coppens, B. B. Xavier, S. Malhotra-Kumar,
699 H. Westh, M. Pinholt, M. F. Anjum, N. A. Duggett, I. Kempf, S. Nykäsenoja, S. Olkkola,
700 K. Wieczorek, A. Amaro, L. Clemente, J. Mossong, S. Losch, C. Ragimbeau, O. Lund, F.
701 M. Aarestrup, ResFinder 4.0 for predictions of phenotypes from genotypes. *Journal of*
702 *Antimicrobial Chemotherapy* **75**, 3491–3500 (2020).

703 77. A. Carattoli, E. Zankari, A. García-Fernández, M. Voldby Larsen, O. Lund, L. Villa, F.
704 Møller Aarestrup, H. Hasman, *In Silico* Detection and Typing of Plasmids using
705 PlasmidFinder and Plasmid Multilocus Sequence Typing. *Antimicrob Agents Chemother*
706 **58**, 3895–3903 (2014).

707 78. M. V. Larsen, S. Cosentino, S. Rasmussen, C. Friis, H. Hasman, R. L. Marvig, L. Jelsbak,
708 T. Sicheritz-Pontén, D. W. Ussery, F. M. Aarestrup, O. Lund, Multilocus Sequence Typing
709 of Total-Genome-Sequenced Bacteria. *J Clin Microbiol* **50**, 1355–1361 (2012).

710 79. D. Arndt, J. R. Grant, A. Marcu, T. Sajed, A. Pon, Y. Liang, D. S. Wishart, PHASTER: a
711 better, faster version of the PHAST phage search tool. *Nucleic Acids Res* **44**, W16–W21
712 (2016).

713 80. L. Avilan, Assembling Multiple Fragments: The Gibson Assembly. *Methods Mol Biol*
714 **2633**, 45–53 (2023).

715 81. R. Ibarra-Chávez, J. Reboud, J. R. Penadés, J. M. Cooper, Phage-Inducible Chromosomal
716 Islands as a Diagnostic Platform to Capture and Detect Bacterial Pathogens. *Adv Sci*
717 (*Weinh*) **10**, e2301643 (2023).

718 82. L. Biskri, M. Bouvier, A. M. Guérout, S. Boisnard, D. Mazel, Comparative study of class 1
719 integron and *Vibrio cholerae* superintegron integrase activities. *J Bacteriol* **187**, 1740–
720 1750 (2005).

721 83. J. DelaFuente, J. Rodriguez-Beltran, A. San Millan, Methods to Study Fitness and
722 Compensatory Adaptation in Plasmid-Carrying Bacteria. *Methods in Molecular Biology*
723 **2075**, 371–382 (2020).

724

725

726 **Acknowledgements:**

727 We would like to thank Dr. José R. Penadés, Dr. Alfred Fillol-Salom and Dr. James J. Bull for
728 providing phages and strains, and Tamara Barcos for technical assistance. We thank other MBA lab
729 members for critical reading of the manuscript.

730 **Funding:**

731 European Union's Horizon 2020 Marie Skłodowska-Curie grant agreement No 847635 (NK)
732 Universidad Complutense PhD program (AH)
733 Juan de la Cierva program FJC 2020-043017-I (PB)
734 Ministerio de Ciencia, Innovación y Universidades FPU21/03268 (LOM)
735 Ministerio de Ciencia e Innovación Programa Ramón y Cajal RYC2019-028015-I (P.D-C).
736 Ministerio de Ciencia e Innovación PID2020-112835RA-I00 (P.D-C)
737 Ministerio de Ciencia e Innovación Subprograma Miguel Servet CP19/00104 (MG-Q),
738 Instituto de Salud Carlos III (Plan Estatal de I+D+i 2017–2020) (MG-Q)
739 European Research Council (ERC) Starting Grant [803375] (JAE);
740 Ministerio de Ciencia, Innovación y Universidades BIO2017-85056-P (JAE)
741 Ministerio de Ciencia, Innovación y Universidades CNS2022-135857 (JAE)
742 Ministerio de Ciencia e Innovación PID2020-117499RB-100 (JAE)
743 EU HARISSA JPI-AMR program PCI2021-122024-2A (JAE)
744 Comunidad de Madrid Programa de Atracción de Talento 2016-T1/BIO-1105 (JAE)
745 Comunidad de Madrid Programa de Atracción de Talento 2020-5A/BIO-19726 (JAE)
746

747 **Author Contributions:**

748 Conceptualization: JAE
749 Investigation: NK, AH, LOM, PB, TD, PV, FMO, TJ, MG-Q, AC, PD-C.
750 Funding acquisition: JAE
751 Project administration: JAE
752 Supervision: MG-Q, PD-C, JAE
753 Writing Original Draft: NK, AH, JAE.
754 Writing review and editing: NK, AH, DJ, PD-C, MG-Q, JAE.
755

756 **Competing interests:**

757 Authors declare that they have no competing interests.
758

759 **Data and materials availability:**

760 The genome of strain KP5 has been deposited in NCBI GenBank (accession numbers: CP162381-
761 CP162384). All other data are available in the main text or the supplementary materials.
762

763 **List of Supplementary Materials**

764 Materials and Methods
765 Figs. S1 to S8
766 Tables S1 to S3
767 References (67-83)